

Electronic properties of icosahedral systems: Energy spectrum, wave functions, and dc conductance

G. Kasner, H. Schwabe, and H. Böttger

Institut für Theoretische Physik, Otto-von-Guericke-Universität Magdeburg, Postschliessfach 4120, 39016 Magdeburg, Germany

(Received 26 July 1994; revised manuscript received 20 December 1994)

The electronic properties of three-dimensional quasicrystals in the icosahedral Danzer model are calculated by using tight-binding Hamiltonians for a vertex and a center model of a finite system. Results are compared with calculations on the two-dimensional Penrose lattice. The energy spectrum, wave functions, and Fermi-energy dependence of the dc conductance at zero temperature are analyzed. Different types of states are found. Most of the states are not degenerate or weakly degenerate and show low conductance. Some very highly degenerate states have zero conductance suggesting that they are strongly localized. By integrating the zero conductance over the Fermi distribution we show that very small differences in the Fermi energy of the system can cause a completely different temperature dependence of the conductance.

I. INTRODUCTION

Since the discovery of thermodynamically stable face centered icosahedral (FCI) phases of high quality quasicrystals¹⁻³ (such as AlPdMn, AlCuFe), anomalous transport properties have been observed on these materials,⁴⁻¹⁰ such as electrical resistance up to some 10 000 $\mu\Omega\text{m}$, strong dependence of the conductivity on the exact chemical stoichiometry, and a negative temperature coefficient of the resistivity. The mechanism underlying this anomalous behavior is not well understood. Zero magnetic field results were fitted to weak localization theories with spin-orbit scattering and electron-electron interaction.^{5,8} On the other hand, positive magnetoconductance data are in conflict with weak localization theory.⁸ Experimental data of AlCuFe and AlPdMn quasicrystals and approximant phases have been fitted as⁶ $\sigma(T) = \sigma_{4K} + \delta\sigma(T)$, where the σ_{4K} term varies strongly with the composition of the samples, whereas the $\delta\sigma(T)$ term has been found to be independent of the sample. This activated behavior has been interpreted by a hopping mechanism between structural entities separated by about 30 Å.⁶

The existence of a pseudogap near $E = E_F$ (E_F Fermi energy) in analogy to Hume-Rothery alloys is generally accepted and confirmed by *ab initio* calculations.¹¹ It was suggested, that physical properties may sensitively depend on the position of the Fermi energy.^{7,12} This may explain the observed different temperature dependence of the conductance of quasicrystalline and approximant phases of nearly the same stoichiometry.¹⁰ The difference of the Fermi level of these phases is expected to be very small. But this is obviously large enough to change the behavior of the conductance completely.⁴⁻¹⁰

Recent experimental results on the conductivity of high quality FCI-type quasicrystals¹³ show an enhanced insulatorlike electron transport behavior of thermally tuned Al-Pd-Re quasicrystals. These findings add evidence for

quasiperiodic order effects on transport properties of high quality (typical FCI) quasiperiodic systems.

Numerical investigations on 1D (one-dimensional)¹⁴⁻¹⁶ and 2D (Refs. 17 and 18) systems have shown that the eigenstates are critical, that means the decay of the envelope follows a power law. The critical character of these wave functions has been related to the competition of the absence of periodicity, which leads to localized eigenstates, and the *repetivity*¹⁹ (often referred to as Conway's theorem), which causes resonances between equivalent local configurations.

The purpose of this paper is to investigate the conductance of a 3D FCI-type quasiperiodic system. Most of the published results are on 1D (Refs. 14-16) and 2D (Refs. 17 and 18) systems. The density of states (DOS) and eigenstates for a 3D Amman-Kramer lattice have been investigated,²⁰ using Bethe lattices to terminate the finite patches. A smooth DOS and delocalized states have been found on this simple cubic icosahedral (SCI) lattice, which describes the more defective Al-Mn phases. These phases do not exhibit such drastic effects on electronic transport properties as the nearly perfect of FCI type.

We are interested in the character of the states and the temperature dependence of the conductance of our model. Due to numerical limitations, the size of the 3D system is restricted to some thousand atoms. Usage of a finite cluster model raises the question of the influence of the boundary conditions. To study the effect of boundary conditions, we compare the results for semiperiodic 2D Penrose strips¹⁸ and finite strips of 2D Penrose patterns with open boundary conditions. We find that the states in the low energy region are more sensitive to the boundary conditions than those in the higher energy regions. The same behavior is expected for the 3D model. The temperature dependent conductance of the 3D model strongly depends on the position of the Fermi energy, which serves as a parameter in our

study.

The paper is organized as follows: In Sec. II, the structural models are introduced and the basic equations of the multichannel Landauer formula^{21–23} are outlined. The DOS of the different models is discussed in Sec. III as well as the nearest-level spacing distribution $P(s)$ for the icosahedral vertex model. Results on 2D and 3D systems are presented in Sec. IV. Section V contains a short summary and concluding remarks.

II. MODELS AND COMPUTATIONAL PROCEDURE

A. Models

For 2D Penrose lattices (PL), we use widely the same model as Tsunetzugu and Ueda¹⁸ with the only exception of open boundary conditions instead of periodic ones, because we want to study the influence of the boundaries on the conductance. In the case of the Penrose lattice, it is possible to introduce a semiperiodic approximant, which describes the same local atomic configuration as the real PL, except of only two defects per unit cell.

For the 3D model introduced below, different approximants can be constructed. But they all should include typical interesting clusters of a real icosahedral quasicrystals. Such approximants are, however, to large for numerical calculations. Therefore, only open boundary conditions are used for the 3D model. Tsunetzugu *et al.*^{17,18} studied the center model of the PL, where atomic s orbitals are placed at the center of each rhombus and unique hopping integrals are assumed between rhombuses, which share an edge.

In our study, we also consider the vertex model of the PL, where the atomic sites are placed at each vertex and hopping integrals do exist between vertices, which are connected by an edge. Both the center and vertex models are described by a single band tight-binding Hamiltonian, introduced and well discussed in Ref. 17.

We restrict our investigations on 3D quasicrystals (QC) to a small piece of a FCI model proposed by Danzer,²⁴ which consists of a set of four tetrahedra. The shape of the model is a rhombic triacontahedron, which was generated by using deflations rules. It is built up of 120 tetrahedra labeled K (this corresponds to vertex star 21 in the global tiling)^{25,26} and then deflated three times. Usage of this model has two advantages: (i) it is of FCI type like high quality quasicrystals as AlPdMn and AlCuFe, (ii) since the prototiles are tetrahedra with four faces, the center model is the simplest extension of the 2D center model, where also four neighbors of each rhombus are present. In the center model, a single s -like orbital is placed in the center of each tetrahedron, while in the vertex model it lies on the vertices. Nearest neighbors in both the models are defined by tetrahedra touching by the face and by two vertices connected by

an edge of the same tetrahedron, respectively. We use the same parameters as Tsunetzugu *et al.*¹⁷ in order to make the results comparable: site energy $\epsilon_i = 0$ and electron transfer energy between nearest neighbors $v = -1$. This choice of parameters is possibly not very good because the size of the tetrahedra is different, but it should be useful for investigating effects of icosahedral structure qualitatively. Due to numerical restrictions, we use only the third level of deflation yielding 1069 sites in the vertex model and 4343 sites in the center model. Note that lower levels do not provide typical QC structures.

As in Ref. 17, one can obtain some spectral properties of the models without calculation. The coordination number in the center model is 4 at all sites, as in the PL, while in the vertex model this value differs from site to site up to 62. Accordingly, in the first case the eigenvalues lie in the energy interval $E = -4 \dots 4$. Furthermore, the Danzer model shows only 4,6 and tenfold axes of rotation. Therefore, the center model is bipartite, so the DOS and the conductance are symmetric. The vertex model is not symmetric.

B. Computational procedure

To calculate the zero temperature dc conductance Γ , we use the Landauer formula^{21,22}

$$\Gamma = \frac{e^2}{h} \text{tr}(tt^+) \quad \text{or} \quad g = \text{tr}(tt^+), \quad (1)$$

where e is the elementary charge, h is Planck's constant, t is the transmission matrix, tr denotes the trace over open channel, and g is the dimensionless conductance.

Equation (1) describes conductance in terms of elastic scattering properties of the systems. It does not take in account any dissipative processes. Such processes have been included into generalized forms of this formula,^{21,23,27} but here we restrict our study to intrinsic effects of quasicrystalline structures. To investigate transmission properties of a finite system, leads of undisturbed material, being infinitely² long but of arbitrary width, are usually attached to two opposite facets (perpendicular to the x axis) of the scattering system. The scattering system (sample) works as a phase randomizing reservoir of propagating states moving through the system. States with real wave numbers k_x correspond to an open channel, whereas those with a complex k_x to a closed channel. The number of open channels depends on the Fermi energy of the whole infinite system. In a tight-binding description, the sum of open and closed channels is equal to the number of sites of each column or one-atomic layer in the leads perpendicular to the direction of propagation.

It is not so easy to define a proper method of attaching a lead to the complicated surface of the triacontahedron model, since there is no periodic lattice having an appropriate structure. We choose the simple cubic lattice because its eigenstates can be analytically obtained. It can be attached to the surface of the triacontahedron model, as shown in Fig. 1(a) and Fig. 1(b). For the vertex and center model, we use an infinite 4×4 cubic lattice. Note

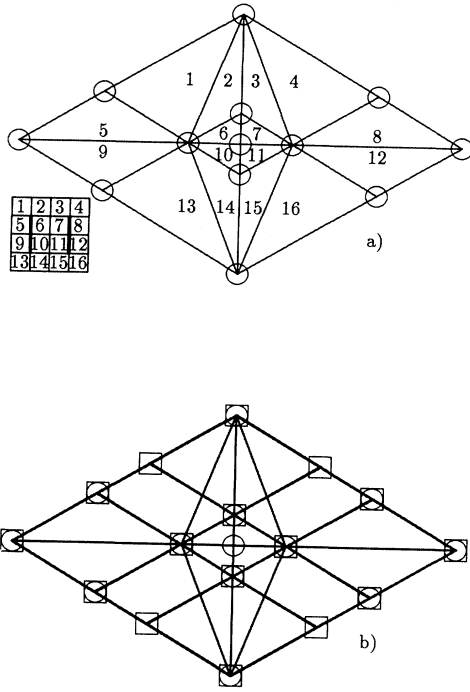


FIG. 1. (a) Connection of a cubic lattice to the facet of the triacontahedron in the center model, third deflation level. Below: the surface at a lead, fat lines denote not connected parts. (b) Connection of a cubic lattice to the facet of the triacontahedron in the vertex model, third deflation level. Circles denote vertices of the quasicrystal, squares are sites of the lead.

that not all sites of the facet at the lead are connected to a site of the lead.

Tsunezugu and Ueda¹⁸ used two methods for calculating the conductance of quasiperiodic model systems in two dimensions. First, transfer coefficients between incident and scattered planar waves were directly determined by solving the Schrödinger equation. This method is very time consuming because a set of linear equations must be solved, whose size is given by the number of sites in the system. Second, the Green function was recursively calculated for a system, which is stepwise built by attaching columns to a half infinite lead. This method was first introduced by Lee and Fisher.²¹ It was suitably modified^{18,28} to be applicable to the Penrose lattice.

The starting point of the latter method is the following expression for the conductance:

$$\Gamma(\omega) = \frac{\hbar}{\pi L^2} \int_{-\infty}^{\infty} dE \sum_{jj'} \text{tr} [J_j \text{Im} G^{\pm}(E + \hbar\omega) \times J_{j'} \text{Im} G^{\pm}(E)] \frac{f(E) - f(E + \hbar\omega)}{\hbar\omega}. \quad (2)$$

Here L is the length of lattice, J_j denotes the current operator of column j , $G(E)$ is the Green function of the system: $G^{\pm}(E) = (E \pm i0^{\pm} - H)^{-1}$, where H is the Hamiltonian, and $f(E)$ is Fermi function, and ω is the frequency of the external electrical field.

For $\omega \rightarrow 0$ and $T \rightarrow 0$, it holds that

$$\lim_{\omega \rightarrow 0} \frac{f(E) - f(E + \hbar\omega)}{\hbar\omega} = - \left. \frac{\partial f}{\partial E} \right|_{E=E_F} = \delta(E_F - E). \quad (3)$$

In this limit, by means of Eqs. (2) and (3), one can obtain the following recursive procedure for calculating g :²¹

$$g = 4v^2 \text{tr}(\tilde{g}_{jj} \tilde{g}_{j+1j+1} - \tilde{g}_{jj+1}^2), \quad (4)$$

where \tilde{g} is the imaginary part of G : $\tilde{g} = -\text{Im}G^+ = \text{Im}G^-$ and

$$G_{jj} = (E\mathbf{1} - \hat{\epsilon}_j - v^2 G_S - \hat{V}_{j-1}^+ G_{j-1}^L \hat{V}_{j-1})^{-1}, \quad (5)$$

$$G_{j+1j+1} = (E\mathbf{1} - \hat{\epsilon}_{j+1} - v^2 G_S - v^2 G_j^L)^{-1}, \quad (6)$$

$$G_{jj+1} = G_{jj} v G_S, \quad (7)$$

$$G_{j'+1}^L = (E\mathbf{1} - \hat{\epsilon}_{j'+1} - \hat{V}_{j'-1}^+ G_{j'-1}^L \hat{V}_{j'-1})^{-1}, \quad (8)$$

$$G_0^L = G_S \quad 1 \leq j' \leq j. \quad (9)$$

Here G^L is the Green function of the left part of the system up to the L th column, $G_{jj'}$ is the jj' -block element of the Green function matrix with the size of the number of sites per column; G_S : Green function of an undisturbed lead column, $\hat{\epsilon}_j$ is the Hamiltonian of the j th column, \hat{V}_j is transfer matrix between column j and $j+1$, and j denotes a column of the right lead.

The necessary prerequisite for this procedure is the possibility of subdividing the system in question into columns of sites, which means that the Hamiltonian can be separated in a tridiagonal block form. There must not necessarily be such an obvious visible geometrical separation of sites, as in the case of a Penrose lattice. Only the first and the last block of the diagonal should correspond to sites of the system, which are connected to the leads. The other diagonal blocks contain sites which are only connected with each other and with sites of the next neighboring blocks and the off diagonal blocks. Thus, we have to solve the problem of a matrix inversion for every block. The corresponding number of numerical operations of an inversion is twice as high as that for the solving a linear set of equations, but the dimension of these matrices, to be inverted, is immensely lower than the dimension of the linear set of the full problem. In order to enhance the effectivity of the computational procedure, we must decompose the system into many small columns. But it is impossible to apply this to the Danzer model because of the very complicated structure of this model. Some very large tetrahedra connect sites located very far from each other. Thus, in the vertex model we get only eight columns, the biggest one of nearly 200 sites. But this fact does not prevent us from using the recursion method. The situation is better for the center model, which can be separated into 34 blocks, the biggest one also includes nearly 200 sites, because the number of tetrahedra exceeds that of the vertices.

III. ENERGY SPECTRUM

A. Density of states

For the icosahedral system, we calculate the exact distribution of the eigenvalues in the center and the vertex model. The DOS for the center model is symmetric around $E = 0$ and has a gap at $E = 0$, as in the vertex model of the 2D PL. There are no large gaps, but the DOS fluctuates over the whole spectrum (cf. Fig. 2).

The DOS of the vertex model extends over the region $E = -18...9$ without gaps. In the negative energy region, there is a flat shoulder (cf. Fig. 3). A similar shape of the DOS has been found for several crystalline approximants using self-consistent calculations¹¹ or in a Hume-Rothery approach.²⁹ There are three highly degenerate states at $E = -1, E = 0$, and $E = 1$. These are states which have nonzero amplitudes only on separate vertex stars (vertex star 1 and 22).²⁵ A detailed investigation of the conductivity shows that these states do *not* contribute to the conductivity.

B. Level spacing distribution

In order to study localization properties of the models, the nearest-level spacing distribution function $P(s)$ (Ref. 30) has been calculated for the 3D icosahedral vertex model. For localized states, $P(s)$ obeys the Poisson law,

$$P(s) = \exp(-s), \quad (10)$$

with $\langle s \rangle = 1$ and crosses over to the Wigner surmise law,

$$P(s) = \frac{\pi s}{2} \exp\left(-\frac{\pi s^2}{4}\right). \quad (11)$$

Recent studies on the metal-insulator transition in 3D Anderson models^{31,32} have shown a continuous crossover from Wigner to Poisson statistics as the disorder increases. A phenomenological one parameter distribution

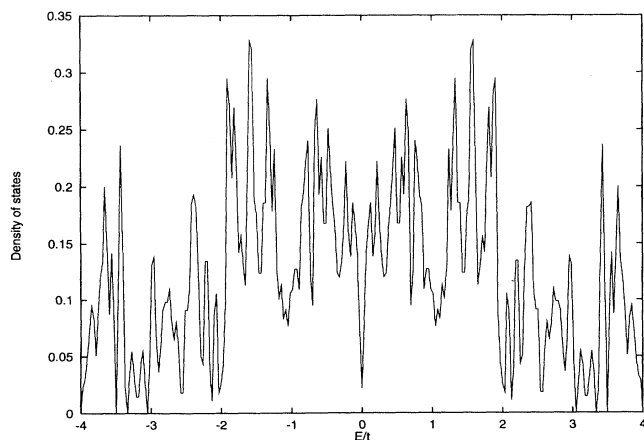


FIG. 2. Density of states for the icosahedral scatterer center model, 4343 atomic sites.

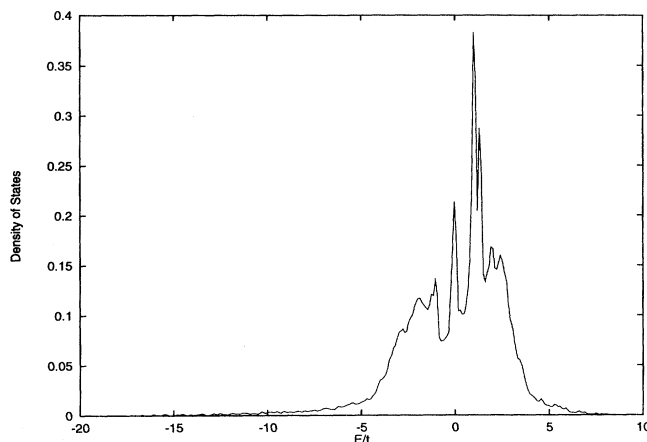


FIG. 3. Density of states for the icosahedral scatterer vertex model, 17 339 sites.

function,

$$P(s) = A s^\beta (1 + C \beta s)^{2\beta(1-\frac{\beta}{2})/\beta-0.16874} \times \exp\left[\left(\frac{\pi s}{4}\right)^2 \beta - \frac{\pi}{2} \left(1 - \frac{\beta}{2}\right) s\right], \quad (12)$$

has been proposed³³ to describe this crossover. The constants A and C in Eq. (12) are determined by normalizing $P(s)$ and the average spacing to unity:

$$\int_0^\infty P(s) ds = 1 \quad (13)$$

and

$$\int_0^\infty s P(s) ds = 1. \quad (14)$$

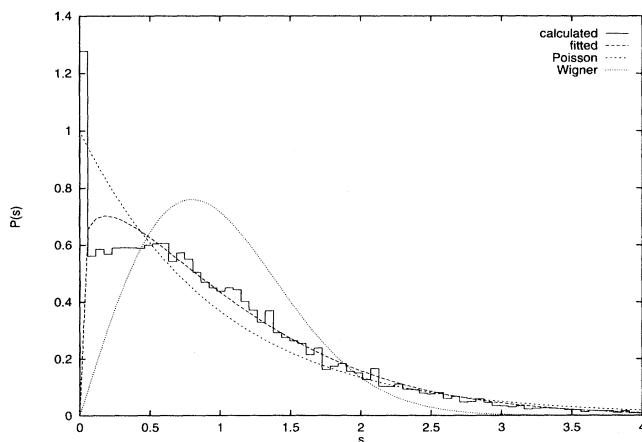


FIG. 4. Level spacing distribution for the icosahedral model with 17 339 sites. The limiting distributions for localized (Poisson) and extended (Wigner) states are also included. The calculated distribution clearly shows a strong tendency to the Poisson distribution, which implies that most of the states are localized. The fitted phenomenological distribution $P(s)$ yields a parameter $\beta = 0.21$.

For $\beta \rightarrow 0$, an expansion of Eq. (12) together with Eqs. (13),(14) leads to the Poisson law [Eq. (10)], which describes localized states. For $\beta \rightarrow 1$ the distribution is nearly that of the Wigner surmise [Eq. (11)], which is valid for delocalized states.

In Fig. 4 the level spacing distribution function for an icosahedral cluster of the vertex model containing 17 339 sites is shown. The peak at $s = 0$ is due to the high degenerate states already mentioned above. A fit to the phenomenological distribution function [Eq. (12)] yields a parameter $\beta = 0.21$. This is a strong indication for our conjecture, that most of the states are localized.

IV. CONDUCTANCE

A. Penrose system

In order to investigate the influence of the boundary conditions to the conductance, we use systems of Penrose approximants of nearly the same size as described in Ref. 18. We calculate the conductance in dependence of the Fermi energy with energy resolution as in the center model in Ref. 18, but with open boundary conditions. Tsunetzugu *et al.*^{17,18,28} found a very spiky dependence of the conductance on the Fermi energy, which has been related to the spiky structure of the DOS. Our results are shown in Fig. 5. We recover the same spiky structure. All peaks can be found at the same value of the Fermi energy and also have nearly the same form as in Ref. 18. The agreement is better in the low energy regions than in the high energy one and increases with increasing site number. For higher energies, and for our smallest system of 65 sites, we find some additional conductance peaks as compared to Tsunetzugu and Ueda.¹⁸ But increasing the size of the system, they vanish rapidly and our curves and the curves of Tsunetzugus and Ueda¹⁸ become more and more the same. This can be explained by realizing that we do not use really the same systems as in Ref. 18. Some different local configurations will lead to a different

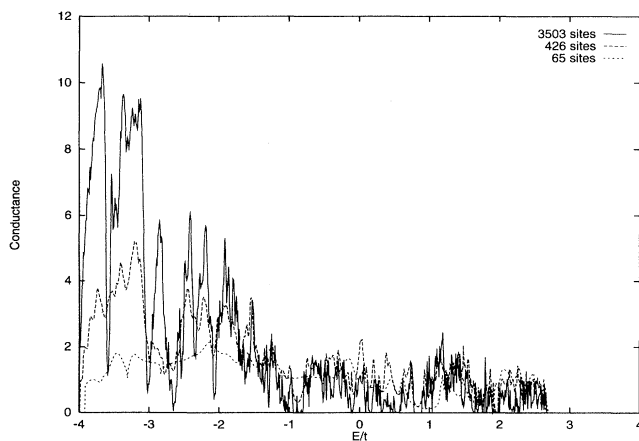


FIG. 5. Conductance as a function of the Fermi energy for Penrose approximants in the center model and open boundary conditions (a) 65, (b) 426, and (c) 3503 sites.

conductance behavior of states at higher energies rather at lower ones, because high energy states are more sensitive for the local structure. The latter one should be more sensitive to the choice of the boundary conditions of the system. With increasing system size, the differences due to boundary conditions and local structure become more and more insignificant. Therefore, the distribution of local structure patterns becomes nearly the same in our systems. That means the influence of the boundary conditions on the conductance is much smaller than that of the system structure. Another argument to show, that states at higher energies should be less sensitive to other influence may be taken from Fig. 6. In addition to the conductance of Fig. 5, the dashed lines are obtained by a modification of the hopping integral v (only in the leads), in order to construct a larger number of open channels at both ends of the energy range. Because of an increasing number of interference possibilities, the conductance becomes more spiky in the low energy region.³⁴ At higher energies, no significant differences to the solid line can be found. That means that these states are influenced mainly by the local structure in a small region. We,

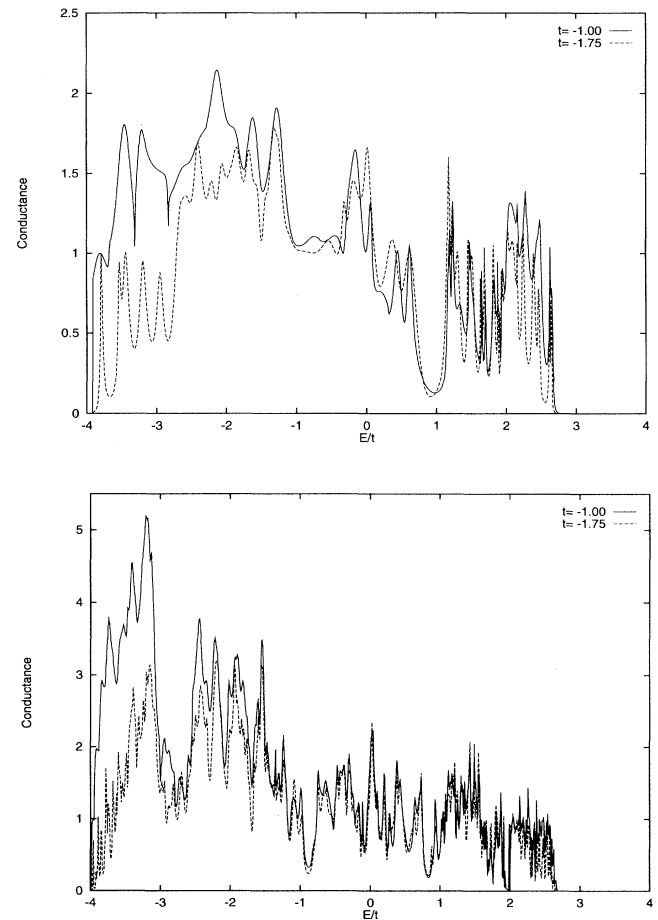


FIG. 6. Conductance as a function of Fermi energy for Penrose approximants in the center model and open boundary conditions, but modified transfer energy in the leads $\epsilon = -1.75$ (dashed line) (a) 65 and (b) 426 sites.

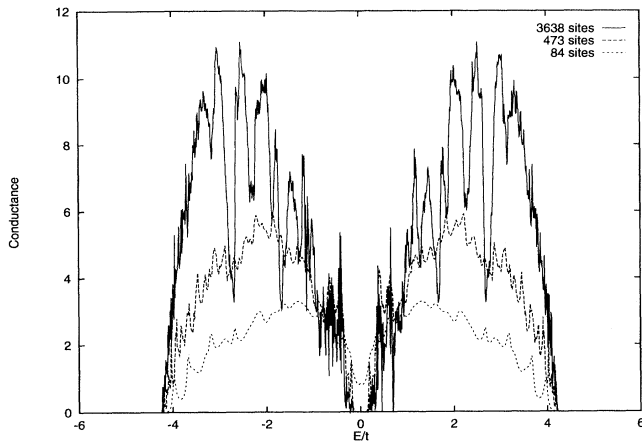


FIG. 7. Conductance as a function of Fermi energy for Penrose approximants in the vertex model and open boundary conditions (a) 84, (b) 473, and (c) 3638 sites.

therefore, conclude that open boundary conditions do not yield other qualitative behavior of the conductance of Penrose systems. So they should be useful for other quasicrystalline systems, especially for the 3D icosahedral model.

Figure 7 shows our results for the vertex model on the same Penrose systems as used for Fig. 5. Once more, the hopping integral v was modified only in the leads in order to construct open channels in the whole band of the scatterer, which extends over the region $E = -7 \dots 7$, because of the maximum coordination number of 7 in these systems. To get the same bandwidth in the leads, we choose $v = -1.75$. Because the Hamiltonian of this system is bipartite, the conductance is symmetric. As in the center model we obtain a spiky structure, which may again be related to the spiky DOS of this model. But as compared to the center model, the strength of fluctuations in the vertex model is independent of the energy region. The wide gap in the center of the energy spectrum can also be found in the conductance. The nonzero conductance observed in this region in our smallest system is a finite size effect, which vanishes with increasing system size. The confined states at $E = 0$ do not contribute to the conductance. Note that there are some asymmetries in theoretically, completely symmetric conductance values caused by numerical rounding errors in the method of matrix inversion and accumulation of these errors at each step of the recursion. This can be seen, for instance, in the largest system in the interval $E = -1 \dots 0$ compared to $E = 1 \dots 0$.

B. Icosahedral system

The results for the conductance in the 3D icosahedral system as described in Sec. II is shown in Fig. 8 for the center model and Fig. 9 for the vertex model. Because of the bandwidth $-18 \dots 9$ of the vertex model, we choose $v = -3.6$ in the leads to get a bandwidth greater than

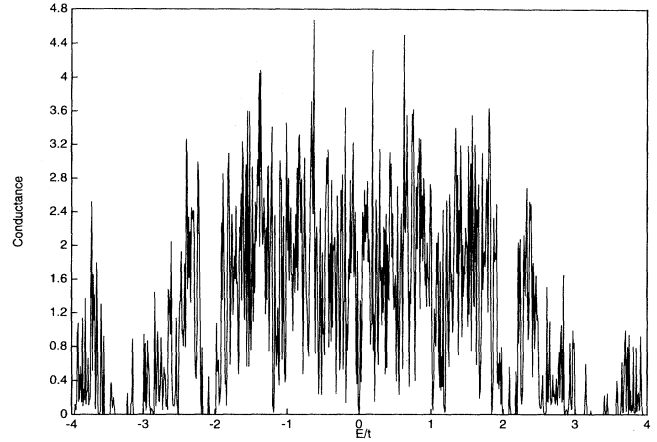


FIG. 8. Conductance as a function of the Fermi energy for an icosahedral scatterer in the center model, third deflation level of the Danzer model. 4343 sites, energy resolution 0.01.

18 in the leads. Because of the very low DOS in the low energy region of the vertex model, we restrict our investigation of the conductance to the more interesting interval $E = -9 \dots 9$ to save computer time. The bandwidth in the center model is 4 and so we can use the same parameter for the leads and the scatterer. We calculate the conductance at Fermi energy values measured in units of the hopping integral v with a resolution of 0.01. We find a spiky structure of the conductance as in the 2D Penrose models. The conductance recovers the DOS (cf. Fig. 2 and Fig. 3), which means that most states should contribute to the conductance of the system. There are some exceptions at the very highly degenerated states at $E = -1, 0$ and 1 in the vertex model. The corresponding confined states do not couple to the system surface and, therefore, they do not contribute to the conductance. The DOS and conductance in the center model are symmetric because of the model is bipartite. Small asymmetries can be explained by accumulation of numerical errors during the recursion. Concerning these asym-

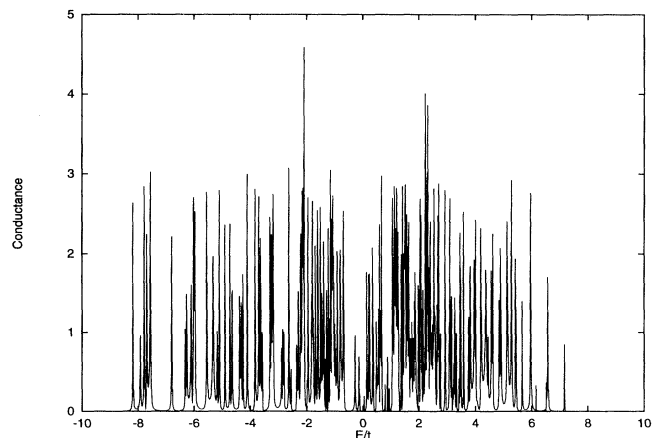


FIG. 9. Conductance as a function of the Fermi energy for an icosahedral scatterer in the vertex model, third deflation level of the Danzer model. 1069 sites, energy resolution 0.01.

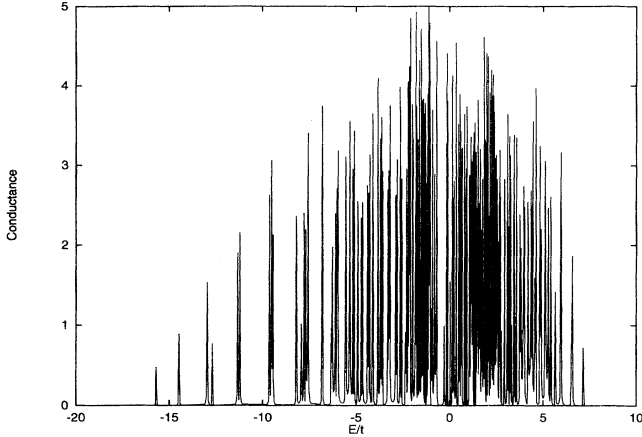


FIG. 10. Conductance as a function of Fermi energy, calculated at seven values, 0.15 units around each eigenvalue of the icosahedral scatterer in the vertex model.

metries, note that we can find nonvanishing conductance only at Fermi energy close to an eigenvalue of the system. The width of one conductance peak is found to be lower than 0.05 energy units. The exact value at a given energy should be extremely sensitive to the distance to an eigenvalue. An equidistant distribution of energy values may lead to a more “stochastic” behavior of the conductance, which depends on its resolution. To eliminate such difficulties, seven energy values were used, which encompass each eigenvalue in a distance of maximal 0.15 units. The result is shown in Fig. 10. In comparison to Fig. 9, the maximum values of conductance peaks are higher because the conductance is calculated at the exact positions of the eigenvalues. A large number of intervals with zero conductance between the high and narrow peaks are found, which are more frequent and narrower in the high energy region. Most of the conducting states lie in an energy interval of $E = -7\dots7$, while at lower energies there

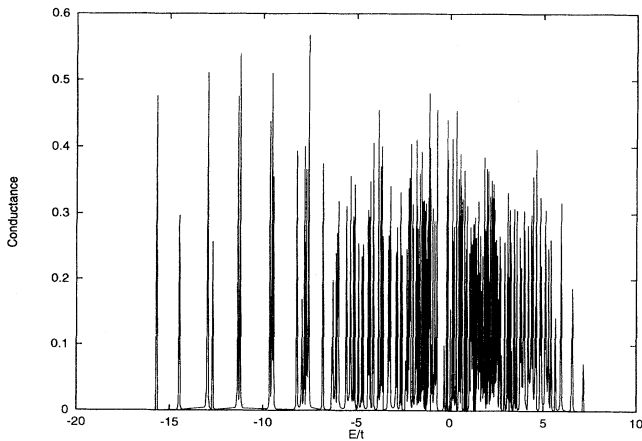


FIG. 11. Conductance as a function of Fermi energy, calculated at seven values, 0.15 units around each eigenvalue of the icosahedral scatterer in the vertex-model normalized to the number of open channels.

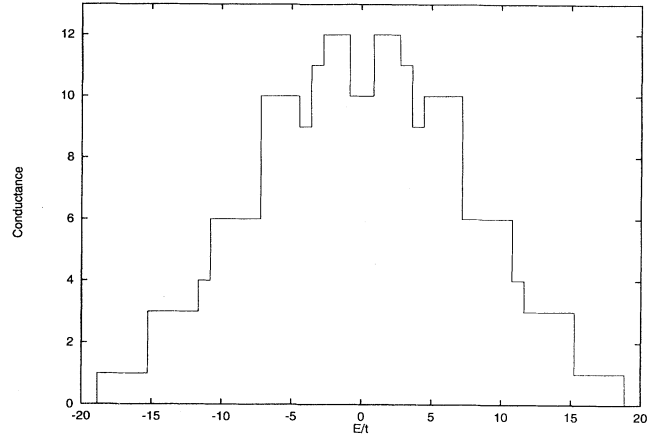


FIG. 12. Conductance of an undisturbed 4×4 cubic lattice.

are only some states within small clusters with large distances in between, as expected from the DOS. Figure 11 is obtained from Fig. 10 by normalizing the conductance to the number of open channels at the energy, which corresponds to that of the conductance of the undisturbed lead system. The conductance for the 4×4 cubic lead is shown in Fig. 12. The conductance per open channel of the states at low energies $E < -7$ seems to be significant higher than that of higher energies.

The temperature dependence of the conductance can be obtained by the integration of the zero temperature conductance multiplied by the first derivative of the Fermi distribution, with respect to E over the energy E . It can be obtained by insertion of Eq. (3) into Eq. (2), which yields

$$\Gamma(\omega) = \int_{-\infty}^{\infty} dE \Gamma(E) \left(\frac{-\partial f}{\partial E} \right). \quad (15)$$

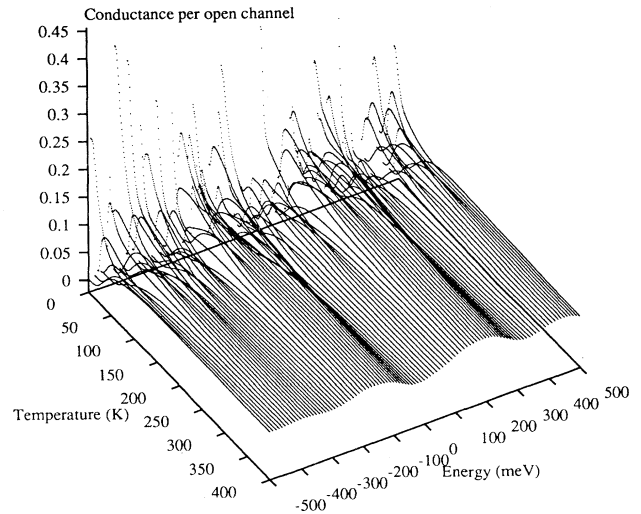


FIG. 13. Conductance per open channel as a function of the Fermi energy and temperature of the system for the icosahedral model.

By choosing the energy units $v = -0.1$ eV, we obtained the conductance as a function of Fermi energy and temperature. The result is shown in Fig. 13 in a 3D plot. By means of this simple model, we can explain the interesting fact that a very small shift of the Fermi energy (for instance, by exchanging some atoms by other ones, by introducing impurities or by using an approximant phase instead of a QC phase) can change the behavior of the conductance completely, as reported by many authors.⁴⁻¹⁰ If the system has a Fermi energy near an eigenvalue, it shows a finite conductance at zero temperature, which decreases with increasing temperature, i.e., such system exhibits metallic behavior. But in the case that the Fermi energy is located in a gap, the conductance is zero and shows an activated temperature. Note that most QC's are reported to show the latter type of behavior (pseudogap at $E = E_F$ due to the Hume-Rothery mechanism^{7,9,11,29}).

V. SUMMARY

In this paper, we have investigated the zero temperature conductance of a 3D model of a FCI quasicrystal in a tight-binding approximation in the center and vertex models. We found a spiky conductance in dependence

of the Fermi energy, which serves as a parameter in our study. The conductance shows rapid changes in temperature dependent behavior if the Fermi energy is varied. We found three highly degenerated states at $E = -1$, $E = 0$, and $E = 1$ in the vertex model. These states have a nonzero amplitude only on special vertex stars, which are not connected with the surface of the model and, therefore, do not contribute to the conductance. Two-dimensional Penrose systems with open boundary conditions were also considered in order to study the influence of the boundaries on the conductance. We found that states in the low energy region are more affected by the boundaries than states at higher energies in 2D as well as in 3D systems. This suggests that the low energy states extend over the whole system. But we cannot conclude that these states are actually extended states, since the system size of our model is possibly too small for such a conclusion.

ACKNOWLEDGMENT

This work was supported in part by the Bundesministerium für Forschung und Technologie under Grant No. 03-BO3MAG-5.

-
- ¹ A. Tsai, A. Inoue, Y. Yokoyama, and T. Masumoto, *Philos. Mag. Lett.* **61**, 9 (1990).
² A. Tsai, A. Inoue, Y. Yokoyama, and T. Masumoto, *Philos. Mag. Lett.* **62**, 95 (1990).
³ C. Beeli, H.-U. Nissen, and J. Robadey, *Philos. Mag. Lett.* **63**, 87 (1991).
⁴ D. Bahadur, A. Das, K. Singh, and A. K. Majumdar, *J. Phys. Condens. Matter* **3**, 4125 (1991).
⁵ H. Akiyama *et al.*, *J. Phys. Soc. Jpn.* **62**, 639 (1993).
⁶ D. Mayou *et al.*, *Phys. Rev. Lett.* **70**, 3915 (1993).
⁷ F. S. Pierce, S. J. Poon, and B. D. Biggs, *Phys. Rev. Lett.* **70**, 3919 (1993).
⁸ M. A. Chernikov, A. Bernasconi, C. Beeli, and H. R. Ott, *Europhys. Lett.* **21**, 767 (1993).
⁹ T. Fujiwara, *J. Non-Cryst. Solids* **153&154**, 390 (1993).
¹⁰ T. Fujiwara, S. Yamamoto, and G. T. de Laissardière, *Phys. Rev. Lett.* **71**, 4166 (1993).
¹¹ T. Fujiwara and T. Yokokawa, *Phys. Rev. Lett.* **66**, 333 (1991).
¹² K. Kimura and S. Takeuchi, in *Quasicrystals: The State of the Art*, edited by D. P. DiVincenzo and P. Steinhardt (World Scientific, Singapore, 1991), p. 313.
¹³ P. S. Pierce, Q. Guo, and S. J. Poon, *Phys. Rev. Lett.* **73**, 2220 (1994).
¹⁴ J. Kollar and A. Sütö, *Phys. Lett. A* **117**, 203 (1986).
¹⁵ T. Schneider, A. Politi, and D. Würz, *Z. Phys. B* **66**, 469 (1987).
¹⁶ B. Sutherland and M. Kohmoto, *Phys. Rev. B* **36**, 5877 (1987).
¹⁷ H. Tsunetzugu, T. Fujiwara, K. Ueda, and T. Tokihiro, *Phys. Rev. B* **43**, 8879 (1991).
¹⁸ H. Tsunetzugu and K. Ueda, *Phys. Rev. B* **43**, 8892 (1991).
¹⁹ L. Danzer, in *Group Theoretical Methods in Physics*, edited by V. V. Dodonov *et al.*, Lecture Notes in Physics Vol. 382 (Springer, Berlin, 1991), pp. 561-572.
²⁰ M. A. Marcus, *Phys. Rev. B* **34**, 5981 (1986).
²¹ P. A. Lee and D. S. Fisher, *Phys. Rev. Lett.* **47**, 882 (1981).
²² A. D. Stone and A. Szafer, *IBM Res. Dev.* **32**, 384 (1988).
²³ S. Datta, *Phys. Rev. B* **47**, 7095 (1993).
²⁴ L. Danzer, *Discrete Math.* **76**, 1 (1989).
²⁵ G. Kasner and H. Böttger, *Int. J. Mod. Phys.* **7**, 1487 (1993).
²⁶ G. Kasner, Ph.D. thesis, Otto-von-Guericke Universität, Magdeburg, 1994.
²⁷ H. M. Pastawski, *Phys. Rev. B* **46**, 4053 (1992).
²⁸ H. Tsunetzugu and K. Ueda, *Phys. Rev. B* **38**, 10109 (1988).
²⁹ G. T. de Laissardière, D. Mayou, and D. N. Manh, *Europhys. Lett.* **25**, 25 (1993).
³⁰ S. N. Evangelou, *Prog. Theor. Phys. Suppl.* **116**, 319 (1994).
³¹ B. I. Shklovskii *et al.*, *Phys. Rev. B* **47**, 11487 (1993).
³² E. Hofstetter and M. Schreiber, *Phys. Rev. B* **48**, 16979 (1993).
³³ G. Casati, L. Molinari, and F. Israilev, *Phys. Rev. Lett.* **64**, 1851 (1990).
³⁴ H. Tsunetzugu, *J. Non-Cryst. Solids* **117/118**, 781 (1990).